Supplementary Information for

"Rational Design of Doubly-Bridged Chromophores for Singlet Fission and Triplet-Triplet Annihilation"

Soichi Ito,[a] Takanori Nagami,[a] and Masayoshi Nakano*[,a,b]

[a] Department of Materials Engineering Science, Graduate School of Engineering Science, Osaka University, Toyonaka, Osaka 560-8531, Japan.

[b] Center for Spintronics Research Network (CSRN), Graduate School of Engineering Science, Osaka University, Toyonaka, Osaka 560-8531, Japan.

*e-mail: mnaka@cheng.es.osaka-u.ac.jp

Tel: +81-6-6850-6265

Table of Contents

Other Possible Phase Patterns for Case (I)

Here we show some possible patterns of the products of MO coefficient of chromophores equivalent to the case (I). When we set the phase of the HOMO (LUMO) of the chromophore 1 multiplied by –1, we obtain an equivalent pattern to the case (I), Table S1 (Table S2). As another case, when we set the phases of the HOMO and LUMO of the chromophore 1 multiplied by –1, we obtain another equivalent pattern to the case (I), Table S3. Like this, there are many seemingly different but physically equivalent phase patterns exist. In the text, we discussed the two simplest patterns shown in Table 1 and 2.

The case for Table S1, where the chromophores are linked with two PC bridges, is schematically shown in Figure S1. In this case, the product of the horizontal couplings is considered to be negative, thus $J_{CT} < 0$, as opposed to the calculated value in the text (**1-(2,2)**, **1-(3,1)** and **1-(3,3)**). However, the sign flip also occurs in J_{Coul}, F_{HL}, and $V_{FE\text{-}TT}$, and hence, the physics does not change totally. Different patterns that represent the same situation in physics with Table S1 are shown in Table S2 and S3.

Table S1. Products (Prefactor in Eq 14) of MO Coefficient of Chromophores Equivalent to the Case (I): the HOMO of the Chromophore 1 Is Multiplied by –1 [a, b]

	H2@b1	H2@b2	L2@b1	L2@b2
H1@b1	–		–	
H1@b2		–		–
L1@b1	+		+	
L1@b2		+		+

[a] H*i*@b*j* (L*i*@b*j*) represents an index of the MO coefficient of the HOMO (LUMO) of the chromophore *i* at the linked site with the bridge *j*, $c_{\mu(j)'\mathrm{H}i}$ ($c_{\mu(j)'\mathrm{L}i}$).
[b] + (–) indicate the positive (negative) sign of the product of MO coefficients of the chromophore 1 shown in the left column and of 2 shown in the top row. Blank cells represent that any signs of the product are possible for these cases.

Table S2. Products (Prefactor in Eq 14) of MO Coefficient of Chromophores Equivalent to the Case (I): the LUMO of the Chromophore 1 Is Multiplied by –1 [a, b]

	H2@b1	H2@b2	L2@b1	L2@b2
H1@b1	+		+	
H1@b2		+		+
L1@b1	–		–	
L1@b2		–		–

[a, b] See Table S1.

Table S3. Products (Prefactor in Eq 14) of MO Coefficient of Chromophores Equivalent to the Case (I): the HOMO and LUMO of the Chromophore 1 Are Multiplied by –1 [a, b]

	H2@b1	H2@b2	L2@b1	L2@b2
H1@b1	–		–	
H1@b2		–		–
L1@b1	–		–	
L1@b2		–		–

[a, b] See Table S1.

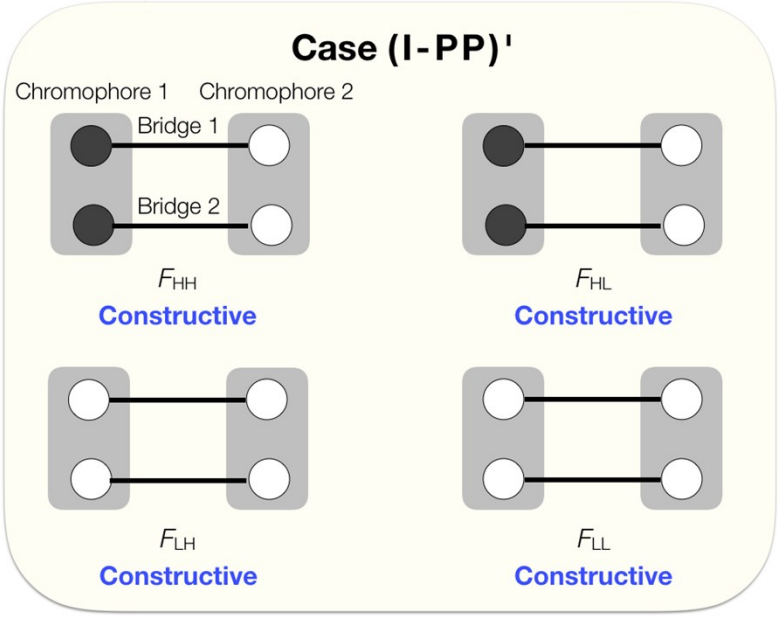

Figure S1. A possible phase pattern (case (I-PP)') that is equivalent to the case (I-PP). This gives the same signs and amplitudes of electronic couplings with those in the case (I-PP), provided the amplitudes of the molecular orbital coefficients are the same.

Definition of Relative Phase of Molecular Orbital

In order to simplify the discussion, we have applied the consistent phase definition for all the molecules. For the series **1-(*m*,*n*)** and **2-(*m*,*n*)**, all these MOs are set to be positive (white) at the linking sites with the bridge 1 in the top view (see Figure S2 and S3 for example). For BET-B, all the MOs are set to be positive at the sites linked with the bridge in the top view (see Figure S4).

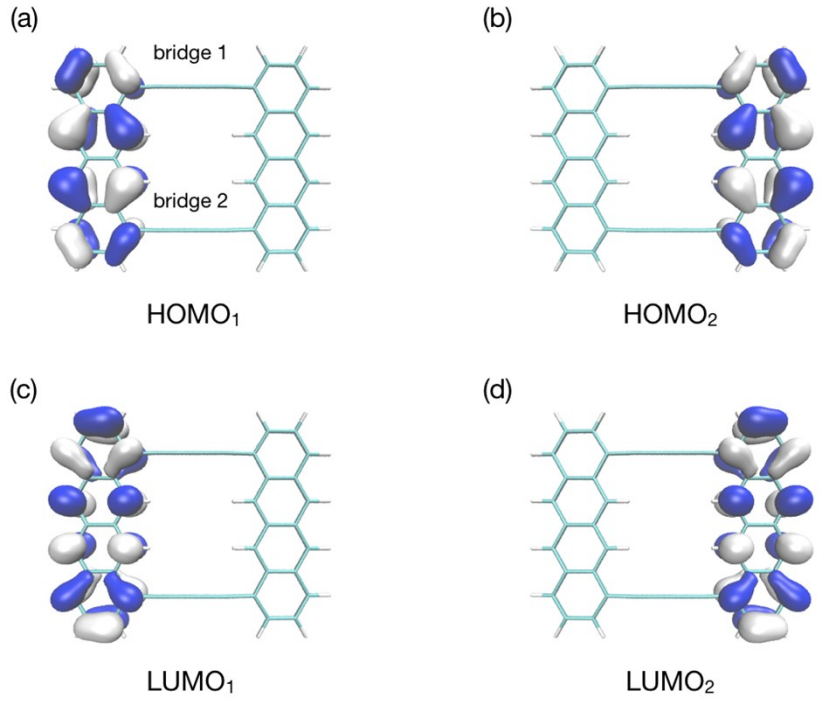

Figure S2. Molecular orbitals of **1-(2,2)**: the HOMO of the chromophore 1 (a) and 2 (b), the LUMO of the chromophore 1(c) and 2(d), respectively. Positive and negative values are represented as white and blue isosurfaces, respectively. Isovalue is ±0.03 au.

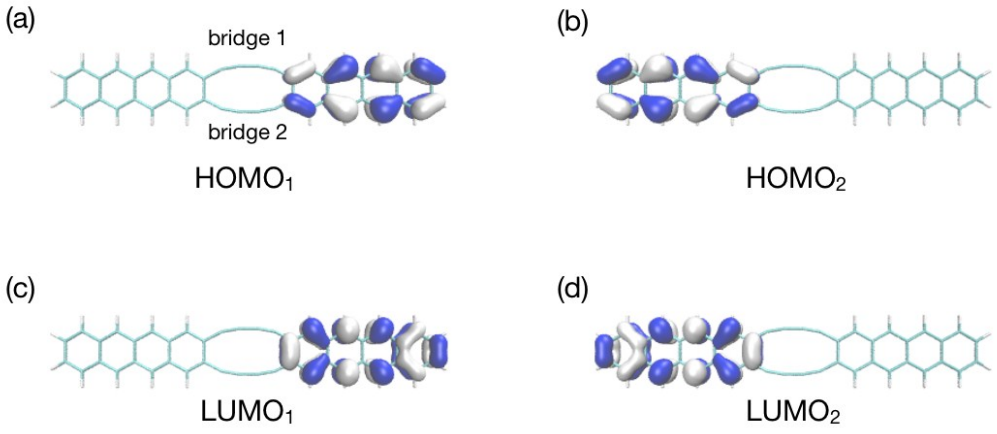

Figure S3. Molecular orbitals of **2-(2,2)**: the HOMO of the chromophore 1 (a) and 2 (b), the LUMO of the chromophore 1(c) and 2(d), respectively. Positive and negative values are represented as white and blue isosurfaces, respectively. Isovalue is ±0.03 au.

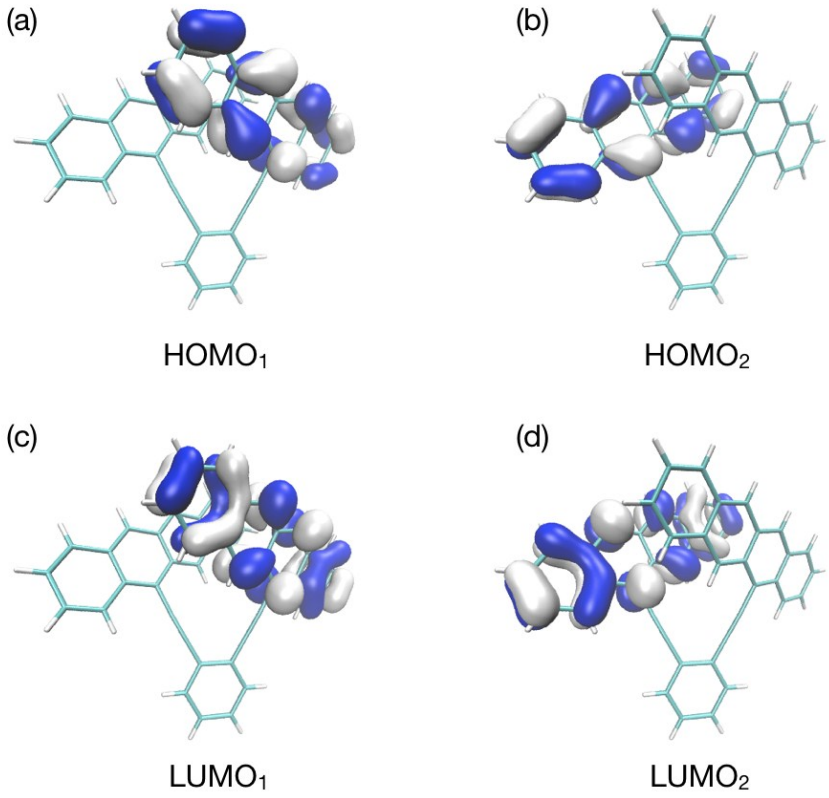

Figure S4. Molecular orbitals of BET-B: the HOMO of the chromophore 1 (a) and 2 (b), the LUMO of the chromophore 1(c) and 2(d), respectively. Positive and negative values are represented as white and blue isosurfaces, respectively. Isovalue is ±0.03 au.

CT State Energy Dependence

Here we present the CT state energy dependence on each CT mediated electronic coupling matrix element estimated from the second order perturbation theory (Figure S5 and S6).

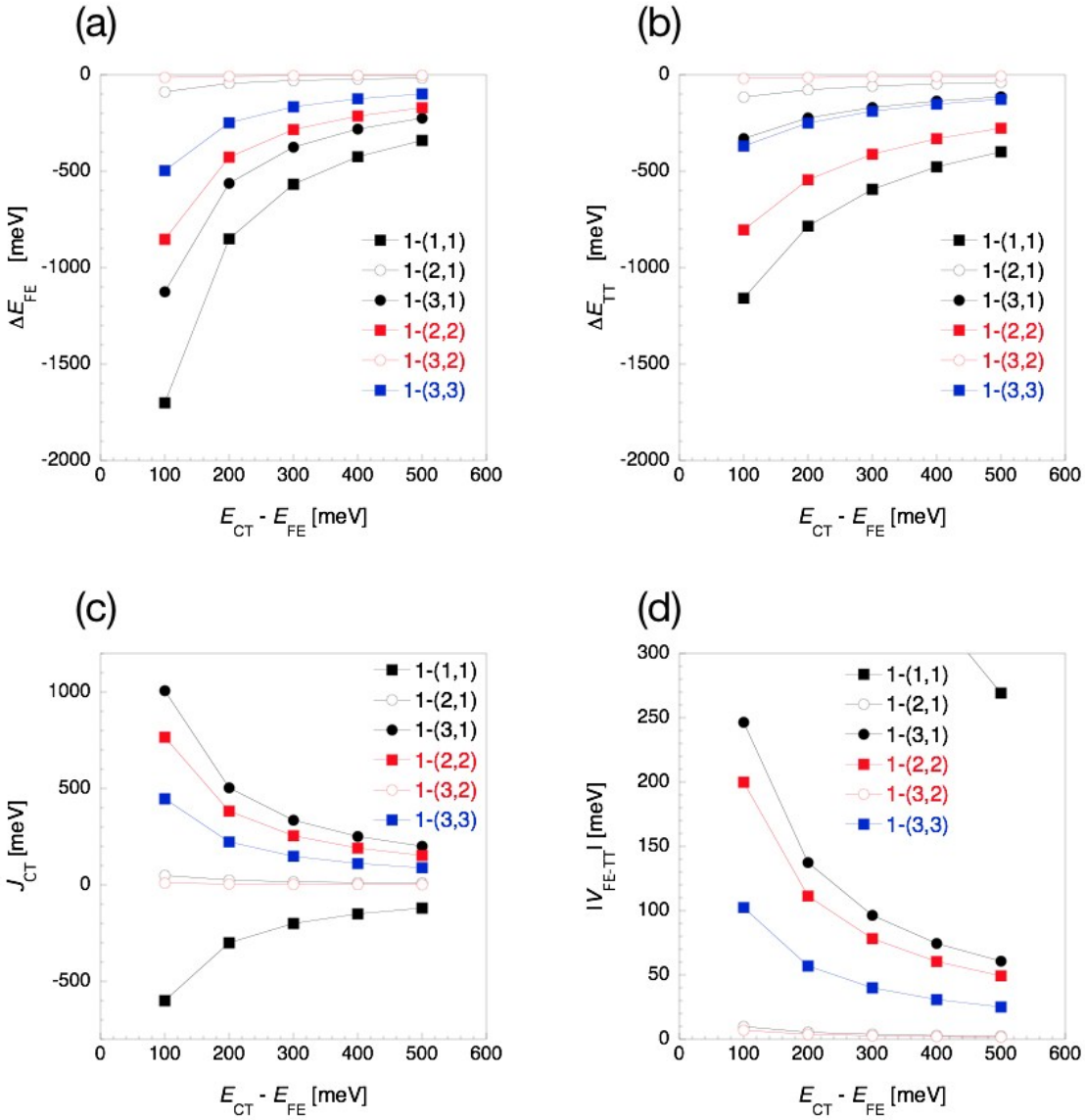

Figure S5. CT state energy dependence of the energy corrections ΔE_{FE} (a) and ΔE_{TT} (b), CT mediated contribution in excitonic coupling J_{CT} (c) and the FE–TT coupling $|V_{FE-TT}|$ (d) of **1-(*m*,*n*)**. Filled and blank markers represent even and odd combinations, respectively. Black, red and blue markers represent n = 1, 2 and 3, respectively. Square and circle markers represent $m = n$ and $m \neq n$, respectively.

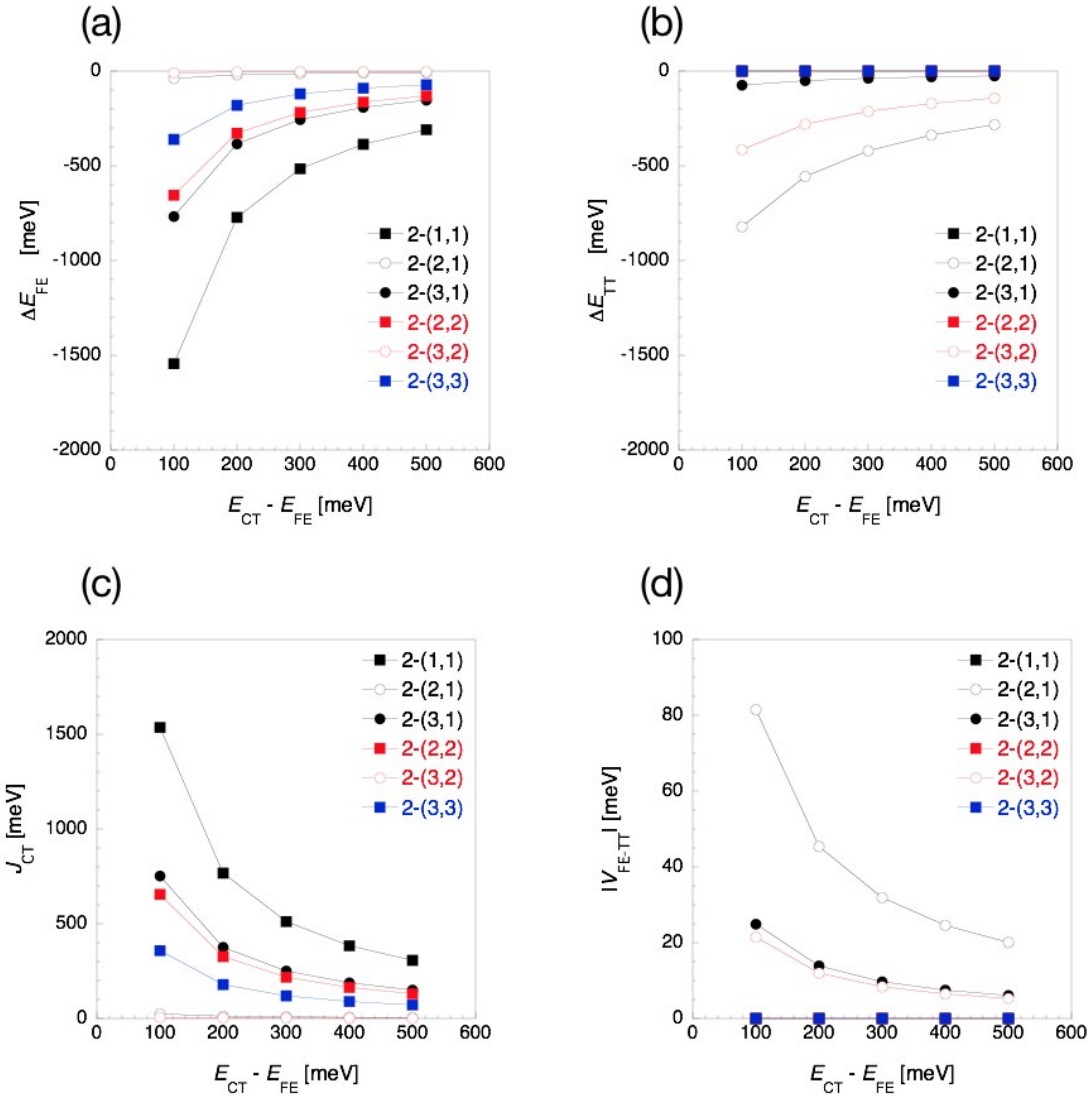

Figure S6. CT state energy dependence of the energy corrections ΔE_{FE} (a) and ΔE_{TT} (b), CT mediated contribution in excitonic coupling J_{CT} (c) and the FE–TT coupling $|V_{FE-TT}|$ (d) of **2-(*m*,*n*)**. Filled and blank markers represent even and odd combinations, respectively. Black, red and blue markers represent n = 1, 2 and 3, respectively. Square and circle markers represent $m = n$ and $m \neq n$, respectively.

Transition Density in Tetracene

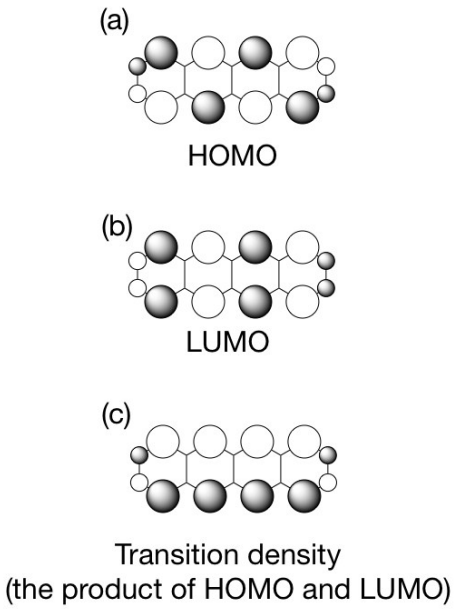

Figure S7. Schematic picture of HOMO (a), LUMO (b) and their product (c) of tetracene.

Decomposition Analysis of Electronic Coupling for BET-B

Here we present the decomposition of the Fock matrix elements of BET-B into the bridge-mediated and direct-overlap contributions (see Figure S8). As seen in the previous study, the bridge-mediated contribution through the ortho-linked conjugated bridge is found to be moderate. The direct-overlap contribution is, however, much larger than those, especially in the non-horizontal couplings F_{HL} and F_{LH}. From this large direct-overlap contribution, BET-B has the strongly stabilized TT state relative to the FE state as pointed out in the text.

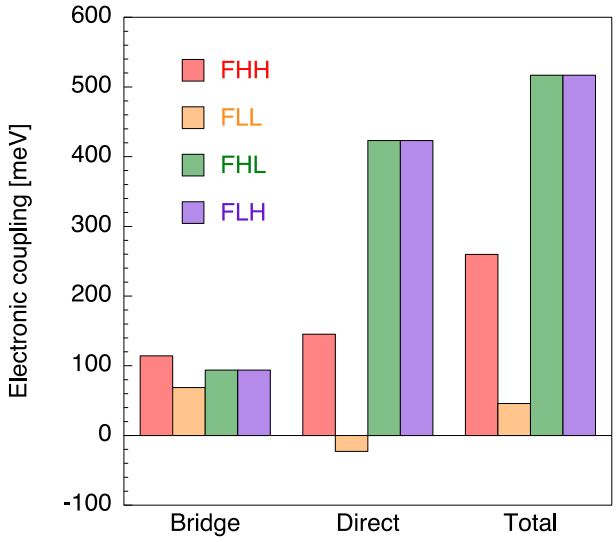

Figure S8. Decomposition analysis of the Fock matix elements in BET-B. Total Fock matrix elements are decomposed into bridge-mediated and direct-overlap contributions.

Proof of Eq 15

We write eq 15 again here as eq S1,

$$(E_{TT} - E_{FE})^{eff} > E_{TT} - E_{FE}. \quad \text{(S1)}$$

This is, of course, not valid in general; nevertheless, it is valid for some special but important cases. First, we assume the covalently-linked dimer is dominated by bridge-mediated contributions in its electronic couplings, F_{ij} and J^{eff}. Second, let the CT state energy be higher than FE and TT state,

$$E_{CT} > E_{TT}, E_{FE} \quad \text{(S2)}$$

Third, let the energy levels of FE and TT states be approximately equal,

$$E_{FE} \sim E_{TT}, \quad \text{(S3)}$$

which may be equivalent for this proof with

$$E_{CT} >> E_{TT}, E_{FE}. \quad \text{(S4)}$$

We consider three cases:

$$\text{(a)} \quad F_{ij} = \beta \text{ for all } i, j \quad \text{(S5)}$$

$$\text{(b)} \quad F_{ij} \sim \beta \text{ for all } i, j \text{ and } F_{HH} > F_{HL} = F_{LH} > F_{LL}. \quad \text{(S6)}$$

$$\text{(c)} \quad F_{HH}, F_{LL} >> F_{HL}, F_{LH} > 0 \quad \text{(S7)}$$

The signs of the Fock matrix elemenst are assumed to be positive for all the elements. In the case (a), the effective energy difference is

$$\begin{aligned}
&(E_{TT} - E_{FE})^{eff} - (E_{TT} - E_{FE}) \\
&= \left(\frac{3}{2}\frac{F_{HL}^2}{\Delta_{CT}} + \frac{3}{2}\frac{F_{LH}^2}{\Delta_{CT}}\right) - \left(\frac{F_{HH}^2 + F_{LL}^2 + 2|F_{HH}F_{LL}|}{\Delta_{CT}}\right) \\
&= \frac{3F_{LH}^2 - (F_{HH} + F_{LL})^2}{\Delta_{CT}} \\
&\overset{\text{case (a)}}{=} -\frac{\beta^2}{\Delta_{CT}} > 0 \ (\because \Delta_{CT} < 0)
\end{aligned}, \quad \text{(S8)}$$

where Δ_{CT} (< 0 from eq S2) is the energy difference between the FE and CT states, or between the TT and CT states (both are considered to be similar in the order of magnitude). In the case (b), we approximate the non-horizontal couplings as

$$F_{HL} = F_{LH} \sim (F_{HH} + F_{LL})/2 \overset{\text{def}}{=} \beta'. \quad \text{(S9)}$$

This can be a good approximation for the case considering the next-nearest-neighbor effect.[1] Then, we obtain

$$\begin{aligned}
&(E_{TT} - E_{FE})^{eff} - (E_{TT} - E_{FE}) \\
&\overset{\text{case (b)}}{=} -\frac{\beta'^2}{\Delta_{CT}} > 0 \ (\because \Delta_{CT} < 0)
\end{aligned}. \quad \text{(S10)}$$

For the case (c), we obtain

$$\begin{aligned}
&(E_{TT} - E_{FE})^{eff} - (E_{TT} - E_{FE}) \\
&\overset{\text{case (c)}}{\sim} -\frac{(F_{HH} + F_{LL})^2}{\Delta_{CT}} > 0 \ (\because \Delta_{CT} < 0)
\end{aligned}. \quad \text{(S11)}$$

Eq S1 has been proved for the cases (a)–(c), at least approximately.

The case (a) corresponds to, for example, bridge-mediated couplind through bridges (either constructive or destructive) evaluated at Hückel level of theory, while the case (b) corresponds to the same situations but evaluated at a higher level of theory including the next-nearest-neighbor interaction such as ab initio molecular orbital theory.[1] The case (b) corresponds to singly-bridged systems[1] and doubly-bridged systems with the cases (I-PP) and (I-PN) as shown in the text. The case (c) correcponds to the case (II-PP) in the text. Eq S1 states that unless the rational design of

bridges or fine control of interchromophore configuration were carried out, which has been demonstrated by the doubly-bridged systems of the case (II-PN) and has also been found in BET-B (see text), the energy requirement for SF in a dimer becomes less exothermic by inter-chromophore couplings than that in a monomer as shown in Figure 7.

Eigenvalues and Eigenvectors of Hamiltonian Eq 1

Exact diagonalization of eq 1 in the text gives the eigenvalues shown in Figure S9. Strong mixing between diabatic states is reflected in large energy splits in even combinations of **1-(*m*,*n*)**, and all bridge patterns of **2-(*m*,*n*)**. On the contrary, the odd combinations of **1-(*m*,*n*)** show very small energy splits.

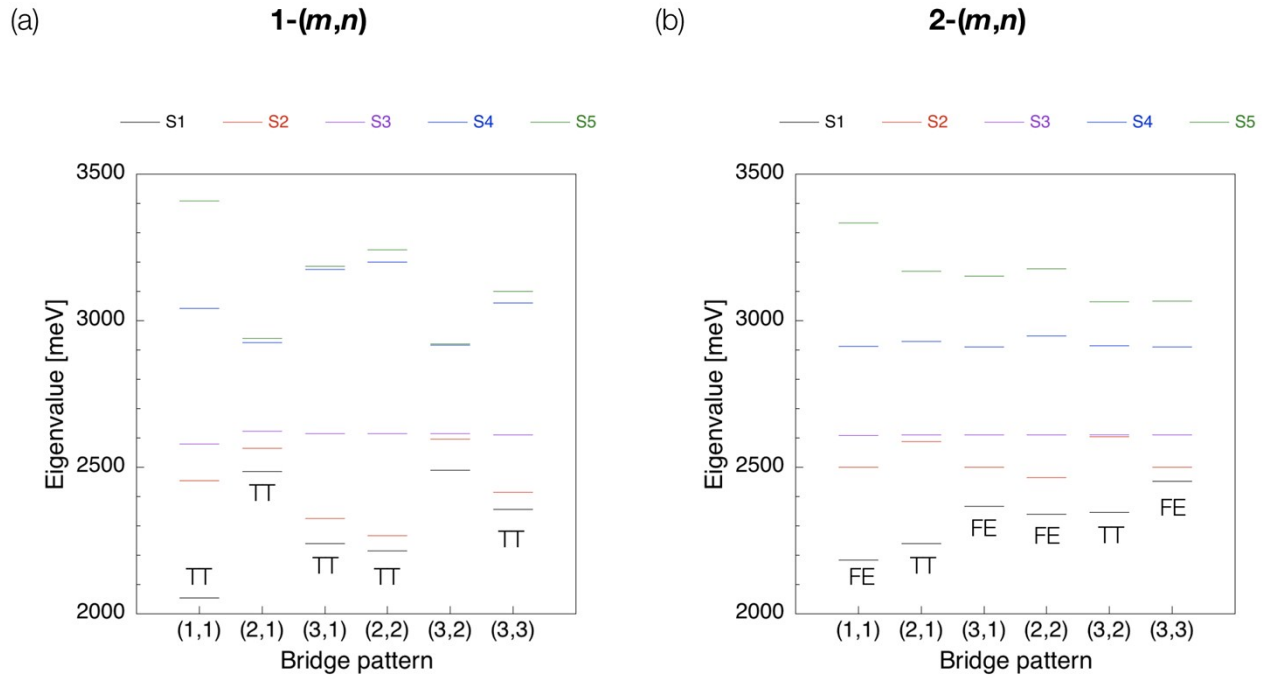

Figure S9. Eigenvalue of eq 1 obtained by the exact diagonalization for (a) and **1-(*m*,*n*)** for (b) **2-(*m*,*n*)**. Main characters of the lowest eigenstates are also described (see also Figure S10).

The main components of eigenvectors are characterized their coefficients. According to the previous study,[2] we define populations of an eigenvector k,

$$p(\mathrm{FE}, k) = |C^k_{\mathrm{S1S0}}|^2 + |C^k_{\mathrm{S0S1}}|^2 \quad \text{(S12a)}$$

$$p(\mathrm{CT}, k) = |C^k_{\mathrm{CA}}|^2 + |C^k_{\mathrm{AC}}|^2 \quad \text{(S12b)}$$

$$p(\mathrm{TT}, k) = |C^k_{\mathrm{TT}}|^2. \quad \text{(S12c)}$$

Calculated populations for the lowest excited state S_1 is shown in Figure S10. In **1-(*m*,*n*)**, the TT character is found to be the primary component in the lowest eigenstate for all (*m*,*n*), while in **2-(*m*,*n*)**, the primary component significantly differs for each. Large TT populations in odd-combinations of **1-(*m*,*n*)** are understood as the results of small mixing between FE and TT diabatic states due to small electronic couplings and lower TT diabatic energy than FE. In **2-(*m*,*n*)**, the even-combinations is turned out to give FE-dominated lowest eigenstates, while the odd-combinations TT-dominated lowest eigenstates. The above findings are in good agreement with the model prediction considered in Section 2, and ab initio calculation results shown in Section 5, except for the even combinations of **1-(*m*,*n*)**. The disagreement in the even combinations of **1-(*m*,*n*)** between perturbative and variational calculations may be attributed to very strong electronic couplings both in horizontal and non-horizontal parts. In such a case, the character of the lowest eigenstate can be a delicate problem (see also Figure 7).

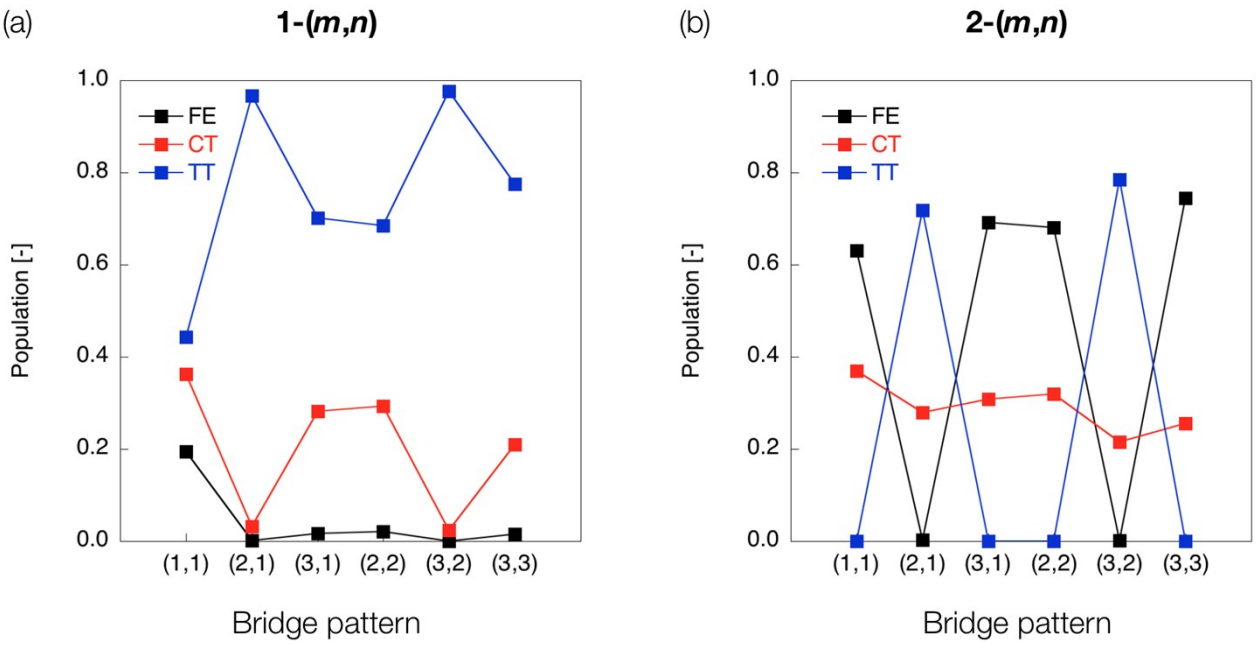

Figure S10. Population of the lowest eigenstates obtained by the exact diagonalization for (a) **1-(*m*,*n*)** and for (b) **2-(*m*,*n*)**.

Detailed Decomposition Analysis of Electronic Coupling in 1-(1,1)

A doubly-bridged chromophore system **1-(1,1)** was found to show significant contributions in its electronic couplings rather than direct contribution and bridge-mediated contribution from π-orbitals of bridges (Figure 5a). Here we further investigate this seemingly strange electronic structure of this molecule.

The molecule **1-(1,1)** has a non-planar structure, that is, distorted π-backbones, belonging to C_{2h} point group. The geometry is graphically shown in Figure S11. This non-planarity is considered as a result of strong nucleus repulsion between hydrogen atoms at the tops of zigzag edges of the chromophores, of which distance is only $R_{H–H}$ = 2.039 Å even in the optimized geometry. The non-planarity of the chromophores caused by H–H repulsion might induce significant σ-π mixing even in the frontier orbitals. The HOMO and LUMO at one of the chromophores that were used as the diabatic basis for electronic coupling calculation are shown in Figure S12. With decreasing the magnitude of isovalue from 0.03 au to 0.01 au, we find that the LUMO does not have pure π-orbital character anymore but should mix with σ-orbitals of bridges and the other chromophore. This is not the case for the HOMO, where π-orbital character seems to be kept.

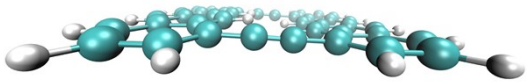

Figure S11. Molecular geometry of **1-(1,1)**. π-Backbone is slightly distorted due to hydrogen-hydrogen repulsion between chromophores.

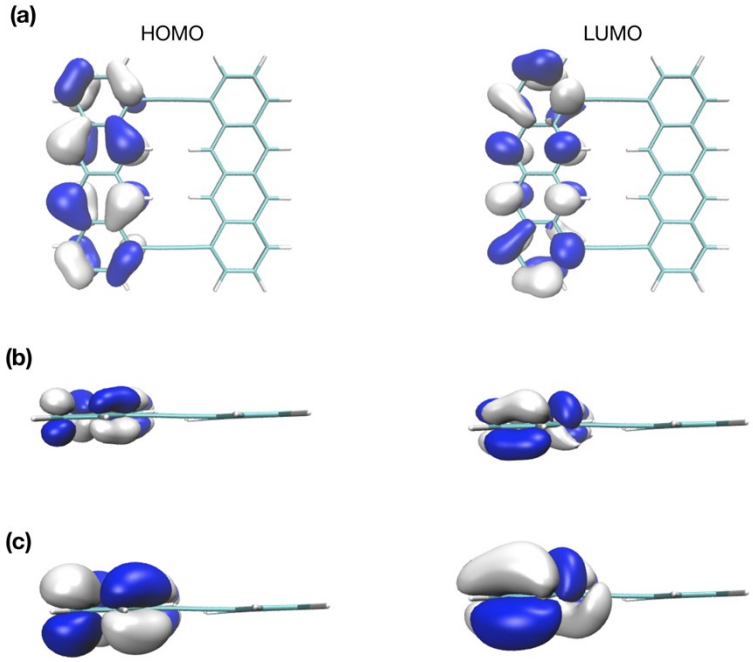

Figure S12. Molecular orbitals of chromophore 1 in **1-(1,1)**: (a) top view with isovalue ±0.03 au, (b) side view with isovalue ±0.03 au, and (c) side view with isovalue ±0.01 au.

In the text, we performed decomposition analysis for electronic couplings in order to investigate the origin of electronic couplings in our model compounds. Here we do this again for **1-(1,1)** with a more detailed way. In the text, we decomposed the orbital space into the π-orbitals of bridge 1, 2 and others. Here we consider the contribution from the following twelve orbital subspaces of which are composed from

(1) bridge core orbitals,
(2) bridge valence σ-orbitals,
(3) bridge valence π-orbitals,
(4) bridge σ-orbitals of higher principle quantum numbers,
(5) bridge π-orbitals of higher principle quantum numbers,
(6) chromophore 1 core orbitals,
(7) chromophore 2 core orbitals,
(8) chromophore 1 valence σ-orbitals,
(9) chromophore 2 valence σ-orbitals,
(10) chromophore 1 valence π-orbitals excluding the HOMO and LUMO,
(11) chromophore 2 valence π-orbitals excluding the HOMO and LUMO,
(12) others (bridge π-orbitals that lie approximately parallel to the molecular plane, bridge δ-orbitals, chromophore σ-/π-/δ-orbitals of higher principle quantum numbers etc.).

Each orbital subspace includes 4, 8, 4, 16, 8, 18, 18, 64, 64, 16, 16 and 460 orbitals, respectively. Note that we do not separate the contributions into that from bridge 1 and from 2, because here we are not interested in quantum interference between bridges but in what kind of orbitals give so large electronic coupling in **1-(1,1)** rather than bridge π-orbitals.

Before going to the decomposition results, we recall the equation considered here. An electronic coupling matrix element described as a Fock matrix element is described as the sum of direct and mediated contributions,

$$\hat{P}^\dagger \hat{F}^{\mathrm{eff}} \hat{P} = \hat{P}^\dagger (\hat{F} - E\hat{I})\hat{P} + \hat{P}^\dagger (\hat{F} - E\hat{I})\hat{G}_{\hat{Q}^\dagger \hat{Q}} (\hat{F} - E\hat{I})\hat{P} \quad \text{(S12)}$$

We focus here only the second term,

$$\langle i|\hat{P}^\dagger \hat{F}^{\mathrm{eff}} \hat{P}|j\rangle^{\mathrm{mediated}} = \sum_{k,l\in Q} \langle i|(\hat{F} - E\hat{I})|k\rangle \langle \tilde{k}|\hat{G}_{\hat{Q}^\dagger \hat{Q}}|l\rangle \langle \tilde{l}|(\hat{F} - E\hat{I})\hat{P}|j\rangle \quad \text{(S13)}$$

To obtain a mediated electronic coupling, we have to sum up all the diagonal blocks of contributions from each orbital subspace (1), (2), ..., (12), and all the off-diagonal blocks of contributions from each pair of orbital subspaces, (1)–(2), (1)–(3), ..., (11)–(12). The off-diagonal blocks may be understood as higher-order terms beyond the second-order perturbation theory from the similarity to a perturbation expansion. Note that the off-diagonal blocks were treated as the rest part ("others") of an electronic coupling in the main text because these were assumed to be very small.

The result of the decomposition analysis using the twelve orbital subspaces for F_{HH} of **1-(1,1)** is presented in Table S4. Table S4 indicates contributions from each orbital subspace both of diagonal and off-diagonal blocks. Off-diagonal part is doubled and shown as the lower triangle part so that the sum of values presented in Table S4 gives the mediated term, eq S13. In spite of non-planatity of the geometry and distorted π-backbones of chromophores, the main contribution to this coupling is clearly dominated from valence π-orbitals of bridges. Off-diagonal blocks have only small contributions, of which magnitude is one or more orders smaller than that of bridge

valence π-orbitals. This confirms that the HOMO of **1-(1,1)** behaves well as a diabatic basis. This agrees our picture obtained from a more simple decomposition that was performed in the text.

In contrast, the twelve orbital subspaces decomposition of F_{LL} indicates a something problematic and non-intuitive behaviour, see Table S5. A significant contribution from bridge valence π-orbitals, 306.9 meV, is what we predicted in Sec 2.3. However, enormous contributions from bridge valence σ-orbitals up to 32 eV (!) in its amplitude is found. Furthermore, contributions from off-diagonal blocks related to bridge core orbitals–bridge σ-orbitals block ((2)–(1)) and bridge core orbitals–chromophore valence σ-orbitals block ((8)–(1), (9)–(1)) are found to have the same order with the previous one. These significant contributions related to σ-orbitals could be understood as a result of the π-backbone distortion in **1-(1,1)**. These contributions almost cancel out and result the total value of –233.8 meV.

Apparently, although a decomposition of F_{HH} helped to confirm our prediction by a simplified model, the same decomposition of F_{LL} gave us little physical insight into the origin of the electronic coupling F_{LL}, especially of contributions rather than bridge valence π-orbitals. This might be attributed to that the LUMO of the chromophores in **1-(1,1)** obtained in this study is not a well-behaved diabatic electronic state. We find such a distorted π-orbital only at the LUMO of **1-(1,1)**, while do not for any frontier orbitals of chromophores. We do not see this kind of problematic behaviour in decomposition analysis for other model compounds. Therefore, we may conclude that strong distortion of π-backbones could reduce physical meaning of diabatic character of the LUMO in the chromophores in **1-(1,1)**, and thus the non-intuitive and physically meaningless interactions was observed. The above discussion gives a caution for diabatic electronic state calculation in a molecule with a distorted π-backbone, especially of related with its LUMO. Finally, we note that a non-planar geometry of a molecule without a distortion in its π-backbone does not induce this kind of problematic behaviour.[1]

Table S4. Decomposition analysis for F_{HH} of 1-(1,1) Evaluated by LC-BLYP/6-31G Level of Theory[a]**

Orbital subspace	1	2	3	4	5	6	7	8	9	10	11	12
1 B core	-0.4											
2 B valence σ	-2.3	0.7										
3 B valence π	-7.4	2.9	336.8									
4 B σ (d)	1.5	0.2	13.8	3.5								
5 B π (d)	1.6	-0.6	-10.6	-1.1	4.7							
6 C1 core	0.0	-0.0	0.0	-0.0	-0.0	0.0						
7 C2 core	0.0	-0.0	0.0	-0.0	0.0	0.0	0.0					
8 C1 valence σ	1.6	-0.2	-1.9	-0.3	0.3	0.0	-0.0	0.0				
9 C2 valence σ	1.6	-0.2	-1.9	-0.3	0.3	-0.0	0.0	-3.2	0.0			
10 C1 valence π	0.0	0.0	-1.9	-0.0	0.4	0.0	0.0	0.0	-0.0	0.0		
11 C2 valence π	0.0	0.0	-1.9	-0.0	0.4	0.0	0.0	-0.0	0.0	0.0	0.0	
12 Others	0.1	0.3	4.5	-0.0	-1.1	-0.0	0.0	-0.6	-0.6	-0.0	-0.0	-0.2

[a] Values in meV. B: bridge 1 and 2, C1: chromophore 1, C2: chromophore 2.

Table S5. Decomposition analysis for F_{LL} of 1-(1,1) Evaluated by LC-BLYP/6-31G Level of Theory[a]**

Orbital subspace	1	2	3	4	5	6	7	8	9	10	11	12
1 B core	3940.3											
2 B valence σ	30380.4	-32250.6										
3 B valence π	-601.4	681.5	306.9									
4 B σ (d)	-376.2	-5157.1	36.6	126.8								
5 B π (d)	264.9	-141.4	8.4	-22.0	21.4							
6 C1 core	-48.4	61.1	-0.5	6.8	-0.0	0.0						
7 C2 core	-46.4	58.5	-0.5	6.5	-0.0	-0.1	0.0					
8 C1 valence σ	-20969.6	23941.7	-139.1	2978.6	-29.6	0.0	-26.7	0.0				
9 C2 valence σ	-20969.6	23941.7	-139.1	2978.6	-29.6	-28.2	-0.2	-9370.5	0.0			
10 C1 valence π	-8.6	18.7	11.2	1.9	-3.6	0.0	-0.0	0.0	-14.2	0.0		
11 C2 valence π	-8.6	18.7	11.2	1.9	-3.6	-0.0	0.0	-14.2	0.0	0.5	0.0	
12 Others	2223.1	-2719.5	33.3	-313.8	-8.6	1.7	1.7	587.6	589.2	0.8	0.8	-36.8

[a] Values in meV. B: bridge 1 and 2, C1: chromophore 1, C2: chromophore 2.

References for Supplementary Information

(1) S. Ito, T. Nagami and M. Nakano *J. Phys. Chem. A* **2016**, *120*, 6236.
(2) S. Ito, T. Nagami and M. Nakano *Phys. Chem. Chem. Phys.* 2017, **19**, 5737.